Biochimica et Biophysica Acta 1788 (2009) 638–649

Contents lists available at ScienceDirect

Biochimica et Biophysica Acta

journal homepage: www.elsevier.com/locate/bbamem

Validation of all-atom phosphatidylcholine lipid force fields in the tensionless NPT ensemble

Justine Taylor [a], Nava E. Whiteford [a,1], Geoff Bradley [b], Graeme W. Watson [a,*]

[a] School of Chemistry, University of Dublin, Trinity College, Dublin 2, Ireland
[b] Trinity Centre for High Performance Computing, University of Dublin, Trinity College, Dublin 2, Ireland

ARTICLE INFO

Article history:
Received 28 August 2008
Received in revised form 7 October 2008
Accepted 13 October 2008
Available online 30 October 2008

Keywords:
Phospholipid bilayer
Molecular dynamics
Simulation

ABSTRACT

A recently defined charge set, to be used in conjunction with the all-atom CHARMM27r force field, has been validated for a series of phosphatidylcholine lipids. The work of Sonne et al. successfully replicated experimental bulk membrane behaviour for dipalmitoylphosphatidylcholine (DPPC) under the isothermal-isobaric (NPT) ensemble. Previous studies using the defined CHARMM27r charge set have resulted in lateral membrane contraction when used in the tensionless NPT ensemble, forcing the lipids to adopt a more ordered conformation than predicted experimentally. The current study has extended the newly defined charge set to 1-palmitoyl-2-oleoyl-*sn*-glycero-3-phosphatidylcholine (POPC) and 1-palmitoyl-2-docosahexaenoyl-*sn*-glycero-3-phosphatidylcholine (PDPC). Molecular dynamics simulations were run for each of the lipids (including DPPC) using both the CHARMM27r charge set and the newly defined modified charge set. In all three cases a significant improvement was seen in both bulk membrane properties and individual atomistic effects. Membrane width, area per lipid and the depth of water penetration were all seen to converge to experimental values. Deuterium order parameters generated with the new charge set showed increased disorder across the width of the bilayer and reflected both results from experiment and similar simulations run with united atom models. These newly validated models can now find use in mixed biological simulations under the tensionless ensemble without concern for lateral contraction.

1. Introduction

Increasing numbers of membrane-bound protein X-ray structures have opened the door to biomolecular simulations targeting the full membrane environment. Only when proteins are simulated in their native environment can we begin to fully understand the intricate atomic-scale workings of the cell membrane and its influence on biological processes. This task is somewhat daunting but recent increases in computational power have allowed for increasingly elaborate simulations. In even the simplest case we must consider modelling the lipid bilayer as a collection of lipids in various distributions. Thus, to begin on this monumental task we must first have a validated force field for each component in the bilayer.

Lipids have been modelled since the 1980s [1,2] and over the past two decades a significant amount of work has gone into the construction and validation of both single and multiple component bilayers [3–5]. Molecular dynamics simulations of lipid systems are now common place and have been used to explore the physical properties of pure and mixed bilayers [6–11], protein–lipid interactions [12], lipid raft behaviour [13], membrane permeation [14] and biophysical phenomena [15] in general. It has been proposed by several groups that protein–lipid interactions are key in regulating protein functionality [12,16–21], suggesting that the membrane is not simply a place holder for proteins but an integral part of their function. This places a greater emphasis on the reliability of simulated membranes and is reflected by the many force field validation studies performed [22–24].

Accurate force field parameterisation of lipids is not a trivial task and is further complicated by the inherent temperature dependent phase behaviour of lipids [25]. The principal phase in the biological domain is the liquid-crystal or fluid phase (L_α). In this phase lipids maintain a disordered conformation allowing for both their own diffusion and the diffusion of materials through the lipid bilayer. At lower temperatures most lipids will re-organise to form an ordered phase referred to as the gel phase ($L_{\beta'}$). Transition temperatures are well defined for single component bilayers but can vary greatly in mixed systems. The dynamic nature of the fluid phase means that capturing micro- and mesoscale structural detail is experimentally challenging [25]. Current atomistic imaging techniques rely on the generation of static structures over which data can be accumulated. Achieving this without destroying the fluid structure of the membrane or inducing a phase change is a challenge. It is in this regard that molecular dynamics has much to offer the field of membrane research.

* Corresponding author.
E-mail address: watsong@tcd.ie (G.W. Watson).
[1] Current address: Wellcome Trust Sanger Institute, Hinxton, Cambridge, CB10 1SA.

0005-2736/$ – see front matter © 2008 Elsevier B.V. All rights reserved.
doi:10.1016/j.bbamem.2008.10.013

Comparing experimental and simulation data further complicates the validation of new membrane models. While many lipid structures have been experimentally determined, the means by which this is achieved can vary from sample to sample. A review by Nagle and Tristram-Nagle [25] outlines the many techniques which may be used and illustrates the strengths and weaknesses of each. When choosing an experimental value for comparison, ideally, a primary experimental value is used where no assumptions have been made in its interpretation. Experimental diffraction studies in conjunction with Fourier transforms can yield electron density profiles and structure factors, both of which represent primary data. However, comparing simulation data to such experimental quantities is not trivial, requiring Fourier transform of the atomic electron density [26–28]. A simplified approach may be used whereby simple secondary metrics are extracted for comparison to published experimental values. While this comparison is not completely rigorous it does yield tangible atomic level detail which is useful in assessing atom specific effects in newly defined force fields.

Some great successes have been seen in lipid simulation and to a large extent current force fields have been validated. However, progress has mostly been limited to united atom models based on the GROMOS [29,30] force field. Membranes can be reliably simulated in both single and multiple component systems with this group of force fields and a further understanding of membrane behaviour, beyond that afforded by experiment, has been gained. However, to gain a full understanding of lipid–protein or lipid–small molecular interactions a full all-atom force field is required. All-atom models have only been validated under specific ensembles and have seen reduced use because of this. Recent studies have shown there to be certain deficiencies in the CHARMM27r force field [23] when used to model lipids under the isothermal-isobaric ensemble (NPT). Under such conditions individual lipids are seen to adopt an ordered gel phase conformation rather than the expected disordered fluid phase [31]. A similar result has been seen using the Amber GAFF [32] force field combined with RESP charges [33] under NPT conditions [34]. This shortcoming has been overcome using either a fixed membrane surface tension (NPγT) [35,36] or by holding cross-sectional area fixed (NPAT) [37,38]. These methods constrain the models to an acceptable area per lipid value in order to reproduce experimentally observed lipid behaviour. There are several reasons why these constrained ensembles are undesirable. First, the added strain has implications for protein dynamics and diffusion studies. Secondly, simulation in either of these ensembles requires that an accurate area per lipid value be known. This is not trivial and is further complicated when simulating mixed lipid systems. Lastly, it has been argued that the surface tension of flaccid bilayers should be zero [39–41], although this argument has its opponents as well [35,42]. This controversy arises from finite size effects which imply that the small size of the simulation cell suppresses long-range membrane undulations, resulting in decreased area per lipid and a shift to the gel phase. Hence, proponents of this argument believe that a nonzero surface tension is necessary to maintain an acceptable area per lipid [35]. Several simulation studies have shown that this is not entirely true [43,41,44]. Specifically, Wohlert and Edholm [44] reported a contraction in area per lipid of 0.7 $Å^2$ when going from 64 lipids to 1024 lipids in a simulation cell, nowhere near the amount needed to obtain the gel phase. Regardless of any potential finite size effects, it is unclear what effect the introduction of a surface tension will have on protein dynamics in a mixed biological simulation and thus, a force field that functions in the tensionless ensemble is preferred.

Recently, Sonne et al. [31] have proposed an alternative charge set to be used in conjunction with the CHARMM27r force field to model 1,2-dipalmitoyl-*sn*-glycero-3-phosphatidylcholine (DPPC). This new charge set is applied exclusively to the head group atoms and leaves the hydrocarbon tails and all Lennard–Jones parameters to be modelled by the unmodified CHARMM27r force field which is expected to be well defined for hydrocarbons [23]. Analysis of the resulting simulations showed the new charge set to more accurately reflect experimental values for area per lipid and NMR order parameters than the original CHARMM27r force field under NPT conditions. This work aims to extend this approach to two other phosphatidylcholines: 1-palmitoyl-2-oleoyl-*sn*-glycero-3-phosphatidylcholine (POPC) and 1-palmitoyl-2-docosahexaenoyl-*sn*-glycero-3-phosphatidylcholine (PDPC). Both bulk membrane properties and individual atomistic effects were studied and compared to the original CHARMM27r force field. Over the course of this work several membrane analysis tools were developed and have been made publicly available (http://www.tchpc.tcd.ie/moldy).

2. Methods

2.1. Initial structures

Three lipids systems were studied: 1,2-dipalmitoyl-*sn*-glycero-3-phosphatidylcholine (DPPC) [(16:0)(16:0)PC], 1-palmitoyl-2-oleoyl-*sn*-glycero-3-phosphatidylcholine (POPC) [(16:0)(18:1)PC] and 1-palmitoyl-2-docosahexaenoyl-*sn*-glycero-3-phosphatidylcholine (PDPC) [(16:0)(22:6)PC], varying in the degree of saturation of the *sn-2* chain, as shown in Fig. 1. Pre-equilibrated hydrated membrane coordinates were received, with thanks, from the Vattulainen group at

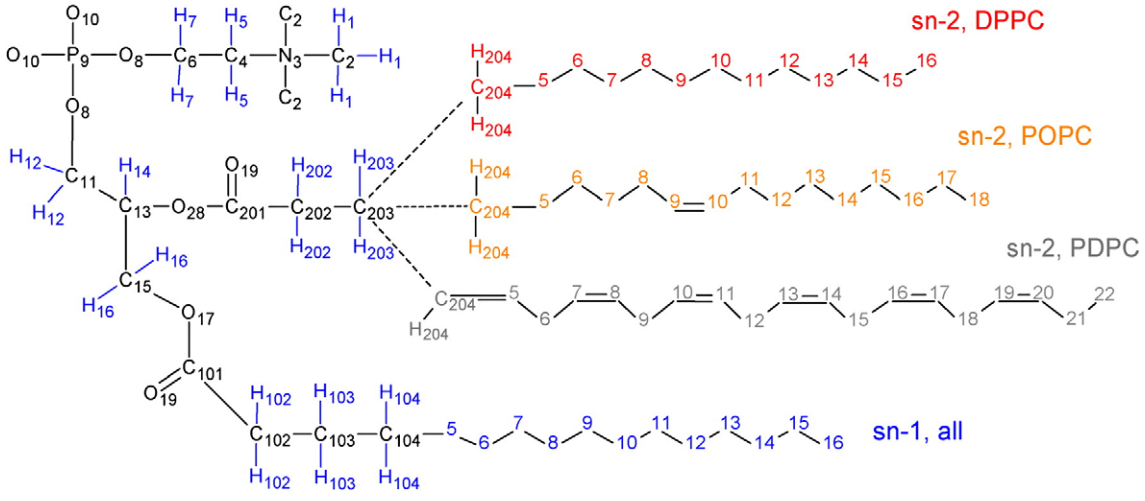

Fig. 1. Lipid structures. All three lipids have the same palmitoyl *sn-1* chain. DPPC has a palmitoyl *sn-2* chain, POPC an oleoyl and PDPC a 2-docosahexaenoyl *sn-2* chain. Throughout this paper the notation Cx# will be used to describe carbons from both *sn* chains. For example, Cx04 refers to both C104 and C204.

the Tampere University of Technology, Finland [45,5,8]. These coordinates were generated using a united atom force field, modelling methyl groups as single carbon based spheres. To allow for the use of an all-atom force field, hydrogens were added using the *Psfgen* plug-in of the Visual Molecular Dynamics program (VMD) [46]. The original simulation cells were replicated and expanded using VMD's *Membrane* plug-in, modified to accept the new membrane coordinates. Each simulation cell consisted of 200 lipids solvated by a 10 Å layer of TIP3P [47] water in the *z*-direction only. This water layer was in addition to the waters retained in the pre-equilibrated coordinates. Solvation was achieved using the VMD plug-in *Solvate* with a solvent boundary of 1.4 Å. Waters were removed from the centre of the membrane and were only allowed to penetrate to the depth originally noted in the pre-equilibrated coordinates. In order to replicate unilamellar vesicle behaviour, as would be most relevant to further membrane-protein simulation, membranes were solvated by approximately 80–90 waters/lipid, well above the swelling limit proposed by Nagle and Tristram-Nagle [25]. The systems were ionised using the VMD plug-in *Autoionise* to a total ionic concentration of 0.2 M using NaCl.

2.2. Force field parameters

All three systems were modelled using a modified version of the CHARMM27 [48,22] force field referred to as C27r [23] (version c32b1), available at http://mackerell.umaryland.edu/CHARMM_ff_params.html. Topology files were constructed for DPPC and PDPC based on parameters included in the original force field, POPC having already been defined. All three systems were modelled with both the original C27r charge set and the new charge set defined by Sonne et al. [31]. Charges were used as defined in Sonne et al. [31] for DPPC and POPC but needed to be slightly altered for PDPC as, in this case, the 4th carbon in the *sn-2* lipid tail is alkenyl as opposed to alkyl. For PDPC, charges were modified down to C104 for the *sn-1* chain but only to C203 for the sn-2 chain (see Fig. 1 for atom names). By not altering C204 a small surplus of charge remains. This was divided among the remaining altered atoms as was the protocol defined by Sonne et al. [31]. Charges are defined in Table 1 for all atoms having modified charges. All other atoms carry the standard C27r charges. Topology files for all three lipids can be found at http://www.tchpc.tcd.ie/moldy.

2.3. Simulation details

All simulations were performed using NAMD 2.6 [49]. The cutoff radius for Lennard Jones interactions was 12 Å with a smooth switching function starting at 10 Å and a non-bonded "pairlist" distance of 14 Å. In all cases periodic boundary conditions were used and the Particle Mesh Ewald (PME) method [50,51] used to evaluate the electrostatics with grid points set no more than 1 Å apart. NAMD's multiple-time-stepping algorithm was used, where bonded interactions were evaluated every 1 fs, short range non-bonded interactions every 2 fs and long-range interactions every 4 fs. Simulations were run over 64 Opteron 250–2.4 GHz AMD 64 bit processors with Infiniband interconnects, achieving approximately 2.2 ns/day.

2.4. System minimisation and equilibration

All systems were initially minimised using 50,000 steps of conjugate gradients. The systems were heated for 50 ps from 0 K to either 310 K (POPC and PDPC) or 323 K (DPPC) under NVT conditions using Langevin dynamics with a damping coefficient of 5 ps^{-1}. The choice of 323 K for DPPC is above the main phase transition temperature for a DPPC bilayer of 314 K [52] and hence it was expected that the lipid would be in the fluid phase. The systems were allowed to relax for 150 ps under NPT conditions maintaining the Langevin damping coefficient at 5 ps^{-1} and using a Nosé-Hoover Langevin [53,54] piston oscillation period of 200 fs and a piston decay time of 100 fs to maintain pressure at 1 atm. The unit cell was allowed to fluctuate anisotropically with the three orthogonal dimensions independent of one another. Finally, the Langevin piston period was reduced to 100 fs, the piston decay time to 50 fs and the simulation continued until equilibrium was achieved. This was determined by monitoring the membrane width, the simulation cell volume and the individual cell dimensions. Total simulation time was 40 ns.

2.5. Analysis

Analysis of the resulting simulations was achieved using several methods. Membrane width and area per lipid calculations were accomplished using the VMD TCL scripting language. Two-dimensional radial distribution function (2D-RDF) calculations were facilitated using the GROMACS [55] *g_rdf* module. All remaining metrics were calculated using in-house C++ tools. In all cases, the membrane was centred in the *z* direction prior to analysis using the average textitz coordinates of the phosphate atoms as the centre point. Averaged properties were calculated over the final 15 ns of simulation, the point at which most membranes had equilibrated. All of the analysis tools used here are freely available at http://www.tchpc.tcd.ie/moldy. Snapshots of the final membrane system were generated using VMD [46] and the provided Tachyon ray tracing library [56]. In

Table 1
Atomic partial charges for C27r and the modified charge set

Atom Name	DPPC/POPC		PDPC		Atom Name	DPPC/POPC		PDPC	
	C27r	Modified[a]	C27r	Modified[a]		C27r	Modified[a]	C27r	Modified[a]
H1	0.250000	0.150668	"	0.152454	H16	0.090000	0.083016	"	0.084802
C2	−0.350000	−0.312617	"	−0.310831	O17	−0.340000	−0.475275	"	−0.473489
N3	−0.600000	0.243851	"	0.245637	O19	−0.520000	−0.600918	"	−0.599132
C4	−0.100000	−0.191031	"	−0.189245	O28	−0.340000	−0.538136	"	−0.536350
H5	0.250000	0.126884	"	0.128670	Cx01[b]	0.630000	0.829360	"	0.831146
C6	−0.080000	0.238693	"	0.240479	Cx02[b]	−0.080000	−0.288139	"	−0.286353
H7	0.090000	0.038553	Same	0.040339	Hx02[b]	0.090000	0.087038	"	0.088824
O8	−0.570000	−0.485323	As	−0.483537	Cx03[b]	−0.180000	−0.015061	"	−0.013275
P9	1.500000	1.300571	DPPC	1.302357	Hx03[b]	0.090000	0.023769	"	0.025553
O10	−0.780000	−0.813248	"	−0.811462	Cx04[b]	−0.180000	0.115859	See below	See below
C11	−0.080000	−0.069093	"	−0.067307	Hx04[b]	0.090000	−0.010607	See below	See below
H12	0.090000	0.097951	"	0.099737	C104			−0.180000	0.117644
C13	0.040000	0.375581	"	0.377367	H104			0.090000	−0.008823
H14	0.090000	0.060207	"	0.061993	C204			−0.150000	−0.150000
C15	−0.050000	0.057803	"	0.059589	H204			0.150000	0.150000

[a] Based on charges provided by Sonne et al. [31].
[b] Where x=1 for the *sn-1* chain and *x*=2 for the *sn-2* chain.

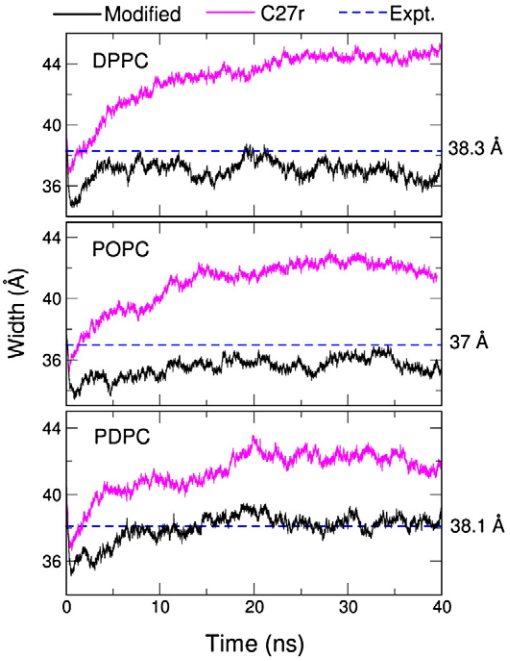

Fig. 2. Membrane width calculated from the average phosphorus positions. Simulations were run at 323 K (DPPC) or 310 K (POPC and PDPC). Experimental results were collected at 323 K for DPPC [25], at 303 K for POPC [72] and at 303 K for PDPC [63].

the resulting plots the solid black trace indicates results of the modified charge set while the purple trace indicates results generated with the C27r charge set.

3. Results and discussion

3.1. Bulk membrane properties

Typically, membrane simulations are thought to have converged when the membrane width becomes stable. The head to head membrane width, D_{HH}, can be expressed as the sum of the hydrophobic thickness, D_C, and the partial head group thickness, D_{H1}, as shown in Eq. (1).

$$D_{HH} = 2D_C + 2D_{H1} \quad (1)$$

Membrane width was calculated as the average distance between head group phosphorus atoms in each leaflet, as an approximation of D_{HH}. The distance between maxima in the total electron density profile is often taken to define D_{HH}, however, this value is significantly harder to monitor over time. Furthermore, recent work has shown there to be little difference between these two values [6]. Experimental values of D_{HH} for DPPC and PDPC were calculated using a determined value of D_C and an estimate for D_{H1} of 9.8–10.4 Å. Whereas, D_C and D_{HH} were determined explicitly through experiment for POPC.

Membrane widths, plotted over the full 40 ns of simulation, are shown in Fig. 2, along with experimental values. When compared to experiment, a large improvement is seen for all three systems using the modified charge set. Stability of the membrane is also improved as widths are seen to reach a plateau value earlier in the simulation, especially in the case of DPPC. Membrane widths averaged over the last 15 ns of the simulations are shown in Table 2. Results generated with the new charge set also compare favourably to a similar study run using a united atom GROMOS based force field [8], (Table 2), from which our starting membrane coordinates were generously provided.

Snapshots of the final membrane structures at 40 ns are shown in Fig. 3. It is immediately apparent that the DPPC simulation modelled with the C27r force field has resulted in highly ordered domains. These ordered domains are most commonly associated with membranes below their melting temperatures (T_m) in the gel phase. The existence of both ordered and disordered domains in the same simulation was also observed by Leekumjorn and Sum [57] and was referred to as a "mixed" domain phase. However, in contrast to the current simulations, which were run at 323 K, the simulations presented by Leekumjorn and Sum [57] were run at temperatures below the main order–disorder transition temperature for DPPC, and hence an ordered phase was expected. The development of an ordered phase above the T_m is, in this instance, indicative of a force field deficiency and has been observed in previous studies [31,58]. In comparison, use of the modified charge set results in a fully disordered structure, in agreement with the results of Sonne et al. [31] using the same charge set for DPPC. Differences between the C27r and the modified charge set for POPC and PDPC are more subtle, and are not discernible through visualisation alone.

To further quantify the membrane structure the lipid distribution across the width of the bilayer was examined, as shown in Fig. 4. The value $\langle N_{mol}(z)\rangle$ was calculated using the average number of non-hydrogen lipid atoms per volume slice taken perpendicular to the membrane normal, i.e. slicing along the z-direction, divided by the number of non-hydrogen atoms per lipid molecule, resulting in the average number of lipid molecules as a function of z. The resulting plot reflects what is seen in Figs. 2 and 3 with the modified charge set resulting in a compression of the lipid layer in the z direction, leading to increased interdigitation and reduction of the "lipid trough" [59]. This effect is most dramatic for DPPC, where the use of the C27r charge set results in a severe loss of lipid density at the membrane centre.

Table 2
Calculated bilayer properties

Method	DPPC (323 K)			POPC (310 K)			PDPC (310 K)		
	Area	D_{HH}	$2D_C$	Area	D_{HH}	$2D_C$	Area	D_{HH}	$2D_C$
	(Å^2)	(Å)	(Å)	(Å^2)	(Å)	(Å)	(Å^2)	(Å)	(Å)
Modified[a]	66.3±0.9	36.9±0.4	27.1	71.2±1.1	35.8±0.5	26.2	69.1±0.9	38.3±0.4	28.5
C27r	49.4±0.4	44.5±0.3	35.3	57.4±0.7	42.4±0.4	31.9	60.6±0.6	42.1±0.4	32.4
GROMOS[b]	65	36	–	68	34	–	71	38	–
Expt.	64[c]	38.3[c,d]	28.5[c]	68.3±1.5[e]	37[e]	27.1[e]	69.2[f]	38.1±0.3[g,h]	28[g]

Averaged over the last 15 ns of simulation. Temperatures are as defined in the header unless indicated otherwise.
[a] Charges defined in Table 1.
[b] From Ollila et al. [8].
[c] From Nagle and Tristram-Nagle [25].
[d] Calculated as $2D_C$+9.8.
[e] From Kučerka et al. [72] at 303 K.
[f] From Koenig et al. [62] at 303 K.
[g] From Petrache et al. [63] at 303 K.
[h] Calculated as $2D_C$+(10.1±0.3).

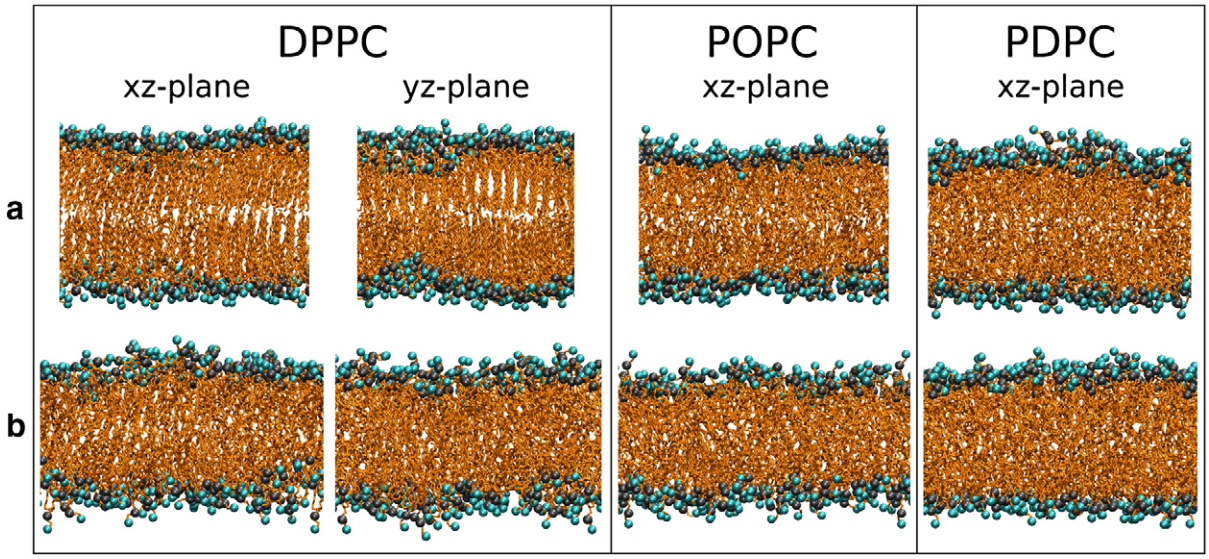

Fig. 3. Snapshots taken at 40 ns for DPPC, POPC and PDPC with the C27r charge set (a) and modified charge set (b). Images were generated using VMD[46] and the Tachyon ray tracing library [56]. Nitrogen atoms are shown in blue, phosphorus in grey and all other heavy atoms in orange.

The spatial distributions of various lipid components across the width of the membrane are shown in Fig. 5. Results are reported as the fraction of total atoms occupied by each group per slice, considering heavy atoms only. In all three systems, use of the modified charge set resulted in increased water penetration, leading to a larger overlap with the carbonyl distribution. This overlap is consistent with a fully hydrated lipid membrane and has been experimentally validated [60,61]. An estimate of the hydrocarbon thickness (D_c) can be made by approximating the full-width at half maximum of the hydrocarbon distribution [25]. This includes contributions from Cx02 to the end of the lipid tail for both chains, including hydrogens (plots not shown). The resulting widths are reported in Table 2 along with experimental estimates. Despite the small discrepancies in temperatures the values obtained with the modified charge set correlate well with the experimental values.

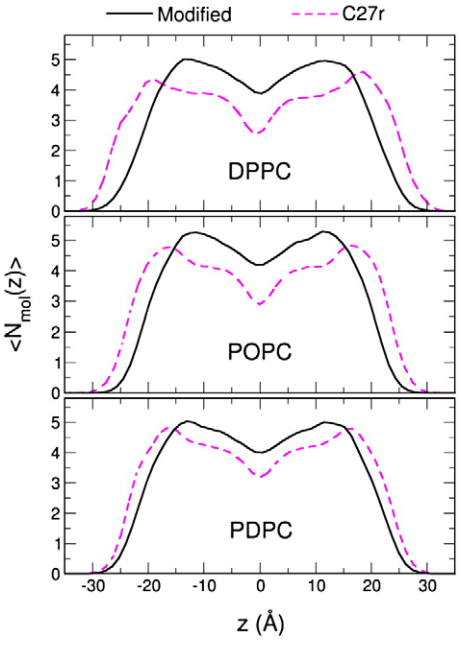

Fig. 4. Average number of lipid molecules as a function of distance from the centre of the bilayer (z).

An important physical property of lipid bilayers, the area occupied per lipid is key to defining bilayer permeability, flexibility and lipid lateral diffusion. It can be determined experimentally with relative ease and thus is a useful metric in lipid force field validation. However, sensitivity to experimental conditions has resulted in a wide range of reported experimental values, suggesting that correlation to experiment should be used as guide and not a definitive measure of success. The experimental values reported here were taken as the most often cited. Area per lipid was calculated as the cross-sectional area of the simulation cell divided by the number of lipids per leaflet. Time dependent results over the entire 40 ns simulations are shown in Fig. 6 and values averaged over the last 15 ns in Table 2. In all cases, the area per lipid for the modified charge set lies closer to the experimental value than that obtained with the C27r charge set. The experimental value taken for comparison with the PDPC simulations was collected for (18:0)(22:6)PC (1-stearoyl-2-docosahexaenoyl-*sn*-glycerol-3-phosphatidylcholine) [62] as no experimental value was available for PDPC, (16:0)(22:6)PC. Based on the work of Petrache et al. [63], it can be assumed that there is little difference between the two values. The values for the modified charge set also compare favourably to work using the united-atom GROMOS based force field, results of which are shown in Table 2. Surprisingly, Sonne et al. [31], who defined the new charge set for DPPC used in this study, reported a value of 60.4 Å^2 for DPPC under nearly identical conditions. This discrepancy may be linked to a lower level of hydration (29 versus 80–90 water/lipids), a shorter simulation time (14 ns versus 40 ns) or to differences in starting structures.

It is important to note the synergy between the aforementioned physical parameters with a view to accurate membrane simulation. Increased area per lipid allows the hydrocarbon tails to move more freely, thus, precluding the development of the “ordered” phase. By allowing the tails to move more freely an increase in leaflet interdigitation is observed resulting in a compression of the hydrocarbon thickness. Furthermore, an increase in area per lipid allows for increased water penetration allowing the hydrophilic head group to become fully saturated. All of these cooperative effects are observed when the new charge set is implemented.

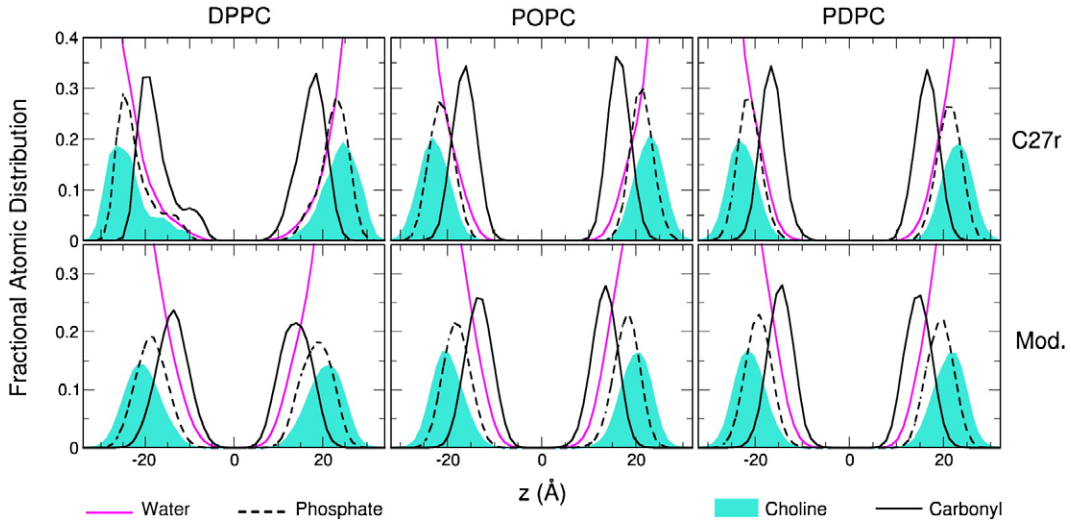

Fig. 5. Atomic distribution as a function of membrane width or *z*, reported as the fraction of total atoms within a volumetric slice for the C27r charge set (top row) and the modified charge set (bottom row).Only heavy atoms were used in the calculation. Choline was defined by NC^3 and water only by O.

3.2. Head group properties

To further assess the impact of the new charge set on lipid behaviour, individual group and atom properties were studied. A number of vector quantities were derived in order to quantify the positions and directionality of the head group atoms. The angular distribution of the P to N vector with respect to the outwards bilayer normal, as shown in Fig. 7a, was seen to shift to smaller angles with the modified charge set. In all cases, the distribution shifts by approximately 7°, from 73° to 66°, resulting in a slightly more upright head group. Experimental estimates of 72° [64] and simulation values of 73° [65] and 78° [8] lend little insight as to whether a more vertical conformation is preferred. The angle between atoms N, P and C13 was calculated, Fig. 7b, in order to help to clarify the results of the P to N angular distribution. In all cases, use of the modified charge set led to a Gaussian distribution centred at 114° whereas the original C27r charge set exhibited a bimodal distribution with a shoulder peak at 80° and main peak at 114°. Use of the modified charges seems to minimise the occurrence of contracted head group conformations leading to, on average, a more extended conformation. This is possibly a result of the reduced electrostatic attraction between the P and N atoms. In the original C27r charge set the choline group carries a +1 charge and the phosphate group a −1 charge. With the new charge set the charges are +0.74 and −0.83 for choline and phosphate respectively, reducing the P–N dipole. This will reduce the attraction between neighbouring lipid headgroups, extending the N_i to P_{i+1} interaction distance and allowing the choline group to extend further into the aqueous phase. This scenario is illustrated in Fig. 8.

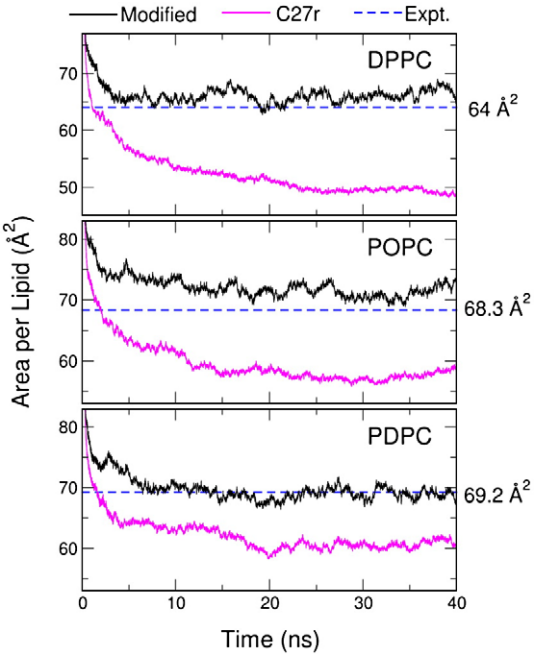

Fig. 6. Area per lipid, calculated by dividing the cross-sectional area of the simulation cell by the number of lipids per leaflet. Simulations were run at 323 K (DPPC) or 310 K (POPC and PDPC). Experimental results were collected at 323 K for DPPC [25] and at 303 K for POPC [72]. A value of 69.2 Å² [62] was determined for (18:0)(22:6)PC at 303 K and can be used for comparison to PDPC, (16:0)(22:6)PC.

The angular distribution of the glycerol backbone vector (C11 to C15) with respect to the inwards bilayer normal also experienced a small shift in distribution, going from approximately 45° using C27r to 51° with the modified charge set (data not shown). This compares favourably to a value of 48°±3° determined from the GROMOS based study [8]. Moving down the lipid backbone, the angular distribution of the vector between the start of the two hydrocarbon chains, C101 to C201, with respect to the outwards bilayer normal is shown in Fig. 7c. Use of the modified charge set results in a shift of the distribution towards 90°, indicating that the tops of the hydrocarbon chains are aligned in the *z*-plane. This is indicative of the relaxed fluid phase. In contrast, use of the original charge set for DPPC resulted in a bimodal distribution shifted towards lower angles, indicating that the carbonyl groups of the two tails were not aligned in the hydrophilic layer. This effect is also seen in Fig. 5 where a side peak is noticeable in the carbonyl distribution for DPPC with the C27r charge set. This peak arises from the rigid conformation of the ordered phase which forces C101 further into the hydrophobic layer than C201.

In order to examine the behaviour of individual atoms in the head group region, 2-dimensional RDF plots were generated for N, P and C13 atoms (each with respect to themselves), as shown in Fig. 9. Only lateral distributions (*xy* plane) were considered in order to clearly illustrate the impact of the variable area per lipid. Of all of the charge modifications made, these three atoms experienced the largest change. Extension of the head group into the aqueous layer serves to decouple its movements from the underlying hydrocarbon layer. Thus, the impact of any hydrocarbon ordering is felt to a lesser extent further from the bilayer centre. Starting with the choline group,

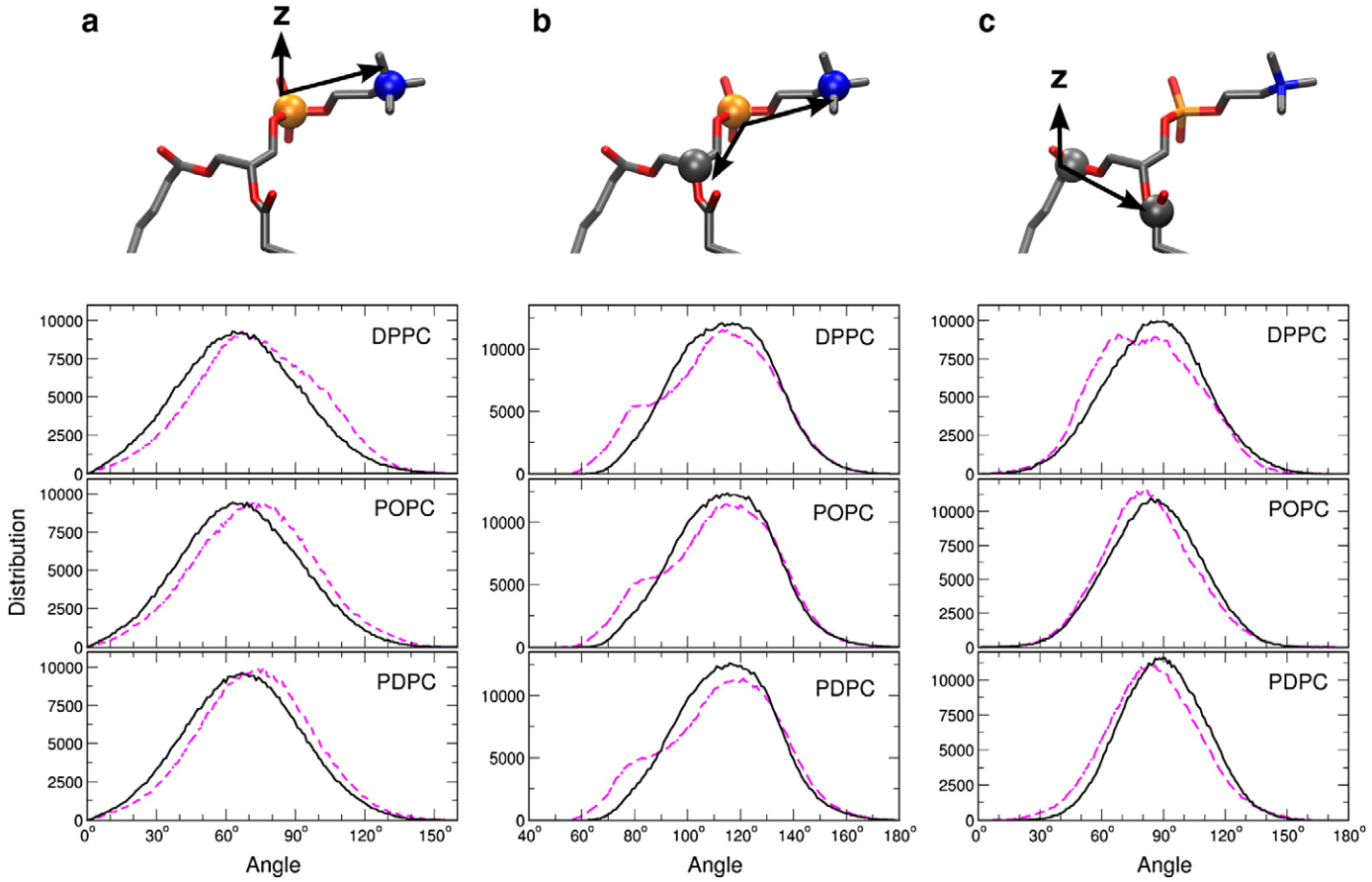

Fig. 7. Head group properties for the C27r charge set (dashed line) and the modified charge set (solid line). (a) Angular distribution of the P to N vector with respect to the outwards bilayer normal. (b) Distribution of the angle formed between atoms N, P and C13. (c) Angular distribution of the vector between the start of the lipid tails, C101 to C201, with respect to the outwards bilayer normal. Atom types are shown in blue(N), red(O), grey(C) and orange(P).

changes in the N to N distributions are subtle, with only a slight shift towards longer coordination distances seen when using the modified charge set. This effect is seen most strongly for DPPC whereas for PDPC there is little difference between the two charge sets. The P to P distributions are slightly less subtle, being closer to the hydrocarbon layer, and show a reduction in order at longer distances with the modified charge set. There is also a reduction in peak maxima and a quicker convergence to $g(r)=1$, indicating a lack of order. The location of C13 at the branching point of the two hydrocarbon tails makes the C13 to C13 distributions more sensitive to hydrocarbon ordering. Results in Fig. 9 for C13 show evidence of ordering in the distribution for DPPC with the C27r charge set. Two peaks are seen at short coordinations distances, reflective of tight hydrocarbon packing. Use of the modified charge set shifts the distributions to larger values dramatically for DPPC and to a lesser extent for POPC and PDPC.

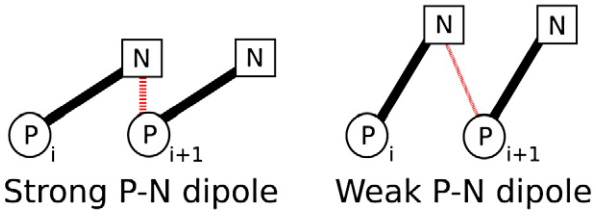

Fig. 8. Schematic of differences in P–N dipoles. A stronger P–N dipole (left) results in a shorter N_i to P_{i+1} distance while a weaker P–N dipole (right) results in a longer N_i to P_{i+1} distance.

Overall, use of the modified charge set results in a reduction of peak maxima and a shift of distributions to longer coordination distances, both indicative of a reduction in order.

3.3. Hydrocarbon chain properties

Although the majority of the charge modifications were made in the head group, atom Cx04 experiences a significant change in charge when compared to the original C27r force field. Sonne et al. [31] have shown that this modification was essential to reproducing accurate membrane behaviour for DPPC. Thus, the following analysis of chain behaviour attempts to explore this requirement.

The relative order of the hydrocarbon tails can be quantified using deuterium order parameters, S_{CD}. These are obtained experimentally via NMR with both selective [66,67] and full [68] deuterium exchange along the lipid tail. They can be calculated from simulation [4] using Eq. (2) where cosθ is the angle between the C_i–H bond vector and the bilayer normal for each carbon along the hydrocarbon tail.

$$S_{CD}^{(i)} = \frac{1}{2}\langle 3\cos^2\theta_i - 1\rangle \qquad (2)$$

Simulation values are shown in Fig. 10 along with experimental results. A larger value of $-S_{CD}$ indicates a higher degree of order. Experimental results for POPC *sn-2* and PDPC arose from dePaked NMR spectra and may not be valid in the low carbon region (i.e. Cx02 to Cx06) [69]. Assignment of dePaked spectra assumes a monotonic decrease of order parameters down the carbon chain resulting in a smooth spectra with a plateau in the low carbon region. This method

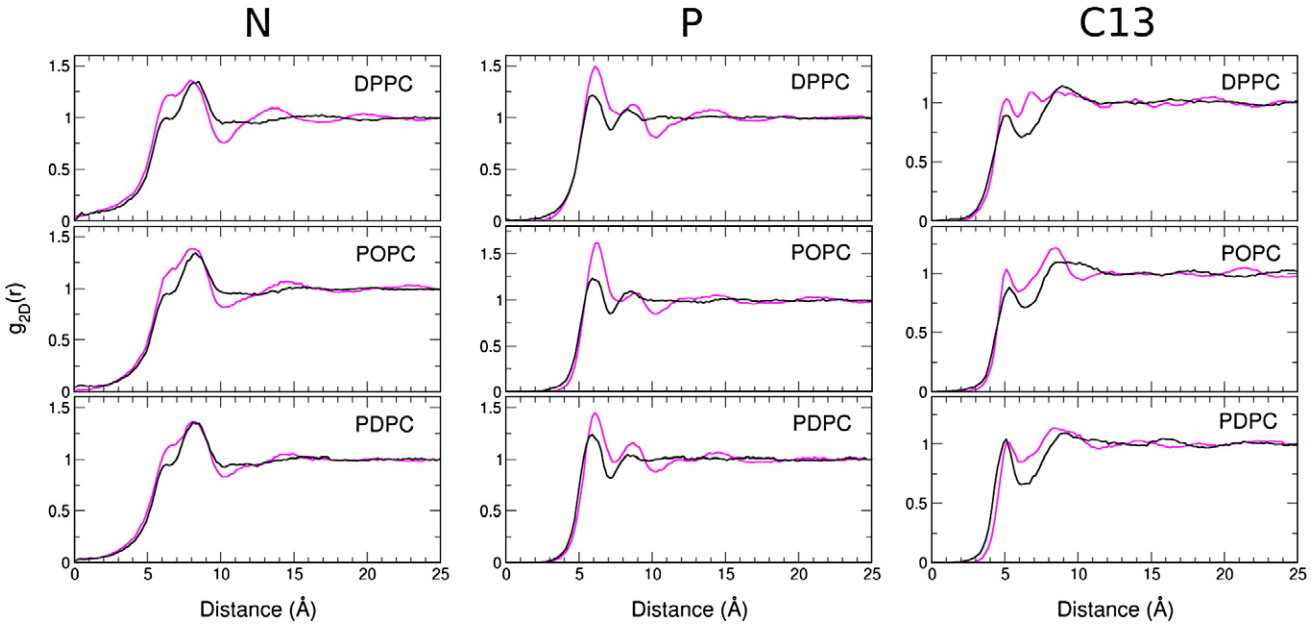

Fig. 9. 2D Radial distribution functions, $g_{2D}(r)$, for N, P and C13 atoms modelled by the C27r charge set (purple or grey) and the modified charge set (black). Only the *xy*-plane is considered in the calculation.

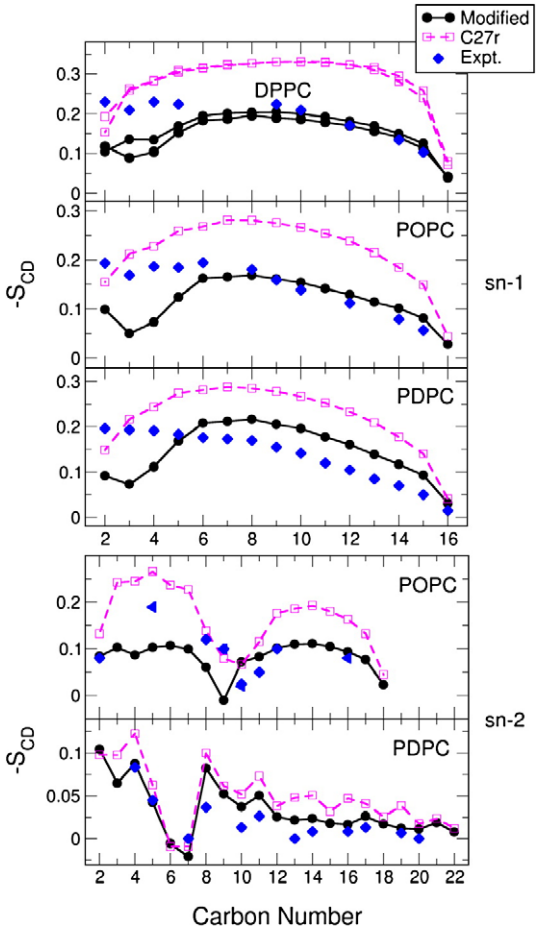

Fig. 10. Deuterium order parameters. Experimental results were collected at 315 K for DPPC [66], at 315 K for POPC *sn-1* [66], at 300 K [73] and 303 K (shown as left triangles) [74] for POPC *sn-2*, extrapolated to 310 K for PDPC *sn-1* [42] and at 303 K for PDPC *sn-2* [42]. Experimental results for POPC *sn-2* and PDPC arose from dePaked NMR spectra.

does not take into account conformational restrictions in the vicinity of the glycerol group, leading to systematic errors in this region. Thus, comparison to experiment in this region using dePaked spectra is somewhat misleading.

In all cases, use of the modified charge set resulted in a significant improvement yielding simulation order parameters in good agreement with experimental results. Results for DPPC were the most pronounced with use of the C27r charge set resulting in highly ordered hydrocarbon tails while the modified charge set led to a more fluid state. Parameters obtained with the modified charge set correlated well to experimental results for Cx05 to Cx16 but were slightly underestimated for Cx02 to Cx04, i.e. less ordered than predicted. This same effect was seen in the work of Sonne et al. [31] under similar conditions and by Rosso and Gould [70] for DMPC, [(14:0)(14:0)PC], using the Amber GAFF [32] force field under NPT. The implications of this increased disorder are unknown. Surprisingly, results collected from a similar simulation using a fixed surface tension (NPγT) [31], were seen to correlate well with experimental results. It is possible that the increased strain of the NPγT ensemble does not allow the membrane structure to fully relax thereby maintaining a false degree of order. If this is the case, one can assume that the strain of this ensemble would also adversely affect protein dynamics if used in a mixed biological simulation. This makes the need for a valid tensionless all-atom lipid force field even greater. The current modified charge set makes some progress towards achieving this goal.

Similar results are seen for the *sn-1* chains of both POPC and PDPC. Once again, carbons closer to the head group appear overly disordered. This result was seen by Huber et al. [42] for PDPC but not for POPC, when using the CHARMM27b5f force field under the NPγT ensemble. Jójárt and Martinek [34] reported overly ordered results using the Amber GAFF force field under NPT and accurate results under the NPγT ensemble, for POPC.

The *sn-2* chain appears to be well represented by the modified charge set, for both POPC and PDPC, with regions of low order occurring between alkene groups. A reduction in order is seen for POPC putting results in line with the sparse experimental findings and closer to results seen with united atom force fields [8]. One issue of contention for the POPC *sn-2* chain is the placement of the alkene dip.

Current results place this dip at C209 using the modified charge set and at C210 using C27r (although the difference is small). Huber et al. [42] places this dip at C209 using CHARMM27b5f under the NPγT, Ollila et al. [8] place it at C210 using an united atom model under NPT, Jójárt and Martinek [34] report it at C209 using GAFF under both NPT and NPγT and experimental results place it at C210. It is unclear where it should actually be, although arguments have been made for both locations. The *sn-2* chain of PDPC is relatively unchanged by the application of the new charge set. The high number of double bonds in this tail implies a highly disordered conformation will be obtained, regardless of the charge set used. Similar results were seen by Huber et al. [42] and Ollila et al. [8], with a large dip at C206–C207 followed by a region of increasing disorder.

The many references to simulation and experimental results in the preceding paragraphs serve to illustrate the wide range of results seen under approximately similar conditions. This begs the question as to where the current results fit into this range. Overall, despite individual atom discrepancies, the general order of the lipid tails has improved with implementation of the new charge set.

To quantify the general movement of the lipid tails, the angular distribution of the tail vectors (vector from Cx01 to the terminal carbon) was calculated with respect to *x*, *y* and *z*. For *x* and *y*, the angle was calculated between the vector and the positive axes only, while for the *z* direction the angle was calculated with respect to the inwards bilayer normal. Starting with the *x* direction, DPPC with the C27r charge set shows a bimodal distribution with peaks either side of 90°, Fig. 11a. This indicates tail directionality and is evident in final snapshots of Fig. 3. The bimodal distribution is indicative of the "tilted ordered" phase [57] where the lipid tails align in a single plane across the entire width of the bilayer including both leaflets. The development of this phase would explain the continuous drift in membrane width seen for DPPC, as the lipids continue to re-arrange, forcing the leaflets further apart. Use of the modified charge set shifts the distribution to a Gaussian centred at 90°, as would be expected for a lipid in the disordered phase. The tilted phase, in this case, is manifest predominately in the *x* direction as only a single narrow peak is seen in the *y* distribution (data not shown). For POPC and PDPC there is no evidence of lipid directionality developing within the time frame studied. In all cases, both for *x* and *y* references, use of the modified charge set serves to broaden the observed angular distributions. This is most likely the effect of an increased area per lipid which allows the tails to move more freely in the hydrophobic layer.

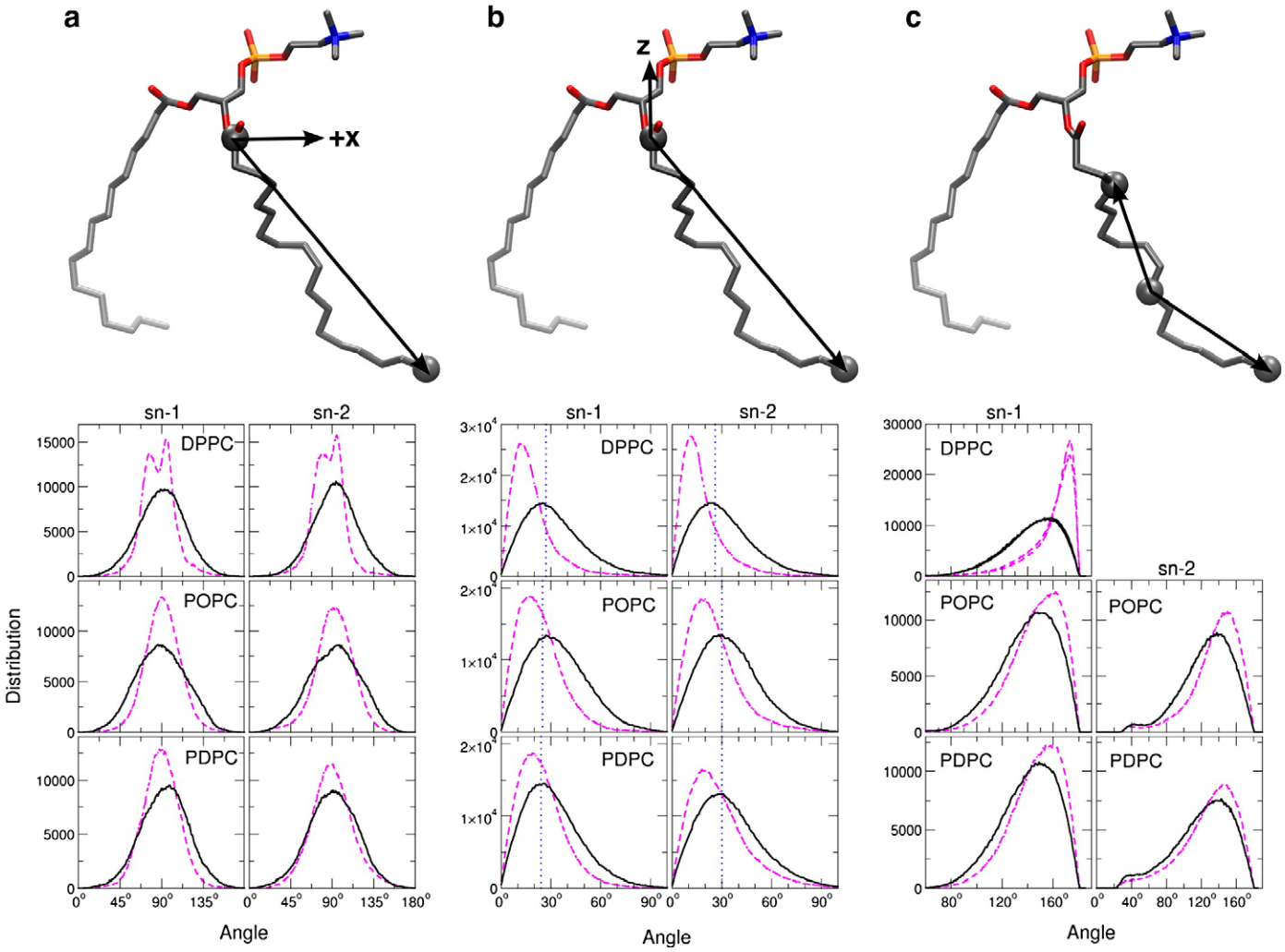

Fig. 11. Angular distributions of the hydrocarbon vectors for the C27r charge set (dashed line) and the modified charge (solid line). Vectors are calculated from Cx01 to the end of the lipid tail for each of the *sn* chains. Angle taken with respect to the positive *x*-axis (a) and with respect to the inwards bilayer normal (b). Included in (b) are the most prevalent angles as reported by Ollila et al. [8] for a GROMOS based simulation (dotted line). For DPPC, POPC and PDPC these were 27°, 25° and 24° for the *sn-1* chain, and 26°, 30° and 30° for the *sn-2* chain, respectively. (c) Distribution of the angle down the *sn* tails. Angles are taken between atoms Cx04–Cx10–Cx16 for DPPC and all *sn-1* chains, between atoms C204–C211–C218 for POPC *sn-2* and between atoms C204–C213–C222 for PDPC *sn-2*. Results for DPPC *sn-1* and *sn-2* are shown in the same plot, top left. Atom types are shown in blue(N), red(O), grey (C) and orange(P).

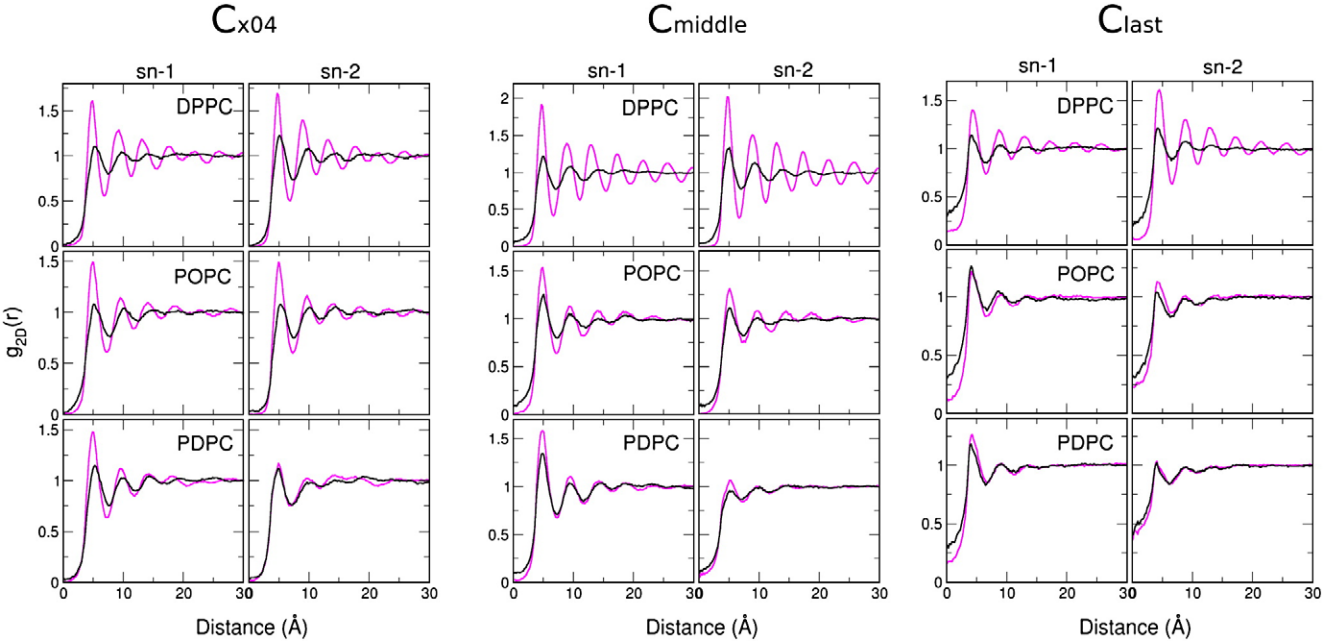

Fig. 12. 2D Radial distribution functions, $g_{2D}(r)$, for Cx04, C_{middle} and C_{last} using the C27r charge set (purple or grey) or the modified charge set (black). C_{middle} is C110 and C210 for DPPC, C110 and C211 for POPC and C110 and C213 for PDPC. C_{last} is C116 and C216 for DPPC, C116 and C218 for POPC and C116 and C222 for PDPC. Only the *xy*-plane is considered in the calculation.

The angular distribution with respect to *z* gives an indication of the vertical nature of the lipid tails. From the snapshots in Fig. 3, a vertical distribution is expected for DPPC with the C27r charge set and this is confirmed in Fig. 11b. All three lipids exhibit a shift in angular distribution to larger angles with the new charge set indicating that the lipid tails adopt a more splayed stance. This has the consequence of decreasing membrane width by allowing the leaflets to approach each other more closely, in turn, increasing the cross-sectional area occupied by a single lipid. Both of these effects were observed earlier. Results with the new charge set correlate well with simulation results from the GROMOS based study [8] which are shown as vertical lines representing the most prevalent angles in Fig. 11b.

The angle adopted by the lipid tails, defined by Cx04–C_{middle}–C_{last}, was calculated to give an indication of overall tail kink. The resulting plots, shown in Fig. 11c, show that, in general, tail kink is increased with the new charge set. A significant change is seen for DPPC when comparing the two charge sets, as would be expected given the vertical nature of the tails seen in Fig. 3 for the C27r charge set. Increased tail kink corresponds to an increased cross-sectional area and is a move towards a fully disordered state.

To lend insight as to individual atom environments, 2D-RDF plots were generated for Cx04, C_{middle} and C_{last}, going down the individual lipid tails. The resulting plots and definitions of "middle" and "last" are shown in Fig. 12. In most cases, use of the modified charge set resulted in reduced maximum intensities and reduced order at longer distances. DPPC is, as expected, the most extreme case with significant amounts of order seen at Cx10 when using the C27r charge set. This was expected based on visual inspection and on the order parameters seen in Fig. 10. Use of the modified charge set shows reduced order for all three atoms and for both chains of DPPC. This effect is less pronounced for POPC, although a reduction of order is seen both at Cx04 and C_{middle} particularly for the *sn-1* chain. RDFs for C_{last} of POPC were relatively insensitive to changes in the charge set. This is an indication of both the disorder expected at the end of the hydrocarbon tail and the disorder introduced by the alkenyl group of the *sn-2* chain. Similarly, only the *sn-1* chain of PDPC shows improvement when using the modified charge set as might have been predicted considering the similarity of the *sn-2* order parameters for PDPC shown in Fig. 10. In this instance, the high degree of unsaturation in the *sn-2* chain mandates that the chain adopts a highly kinked and rigid structure. This enforces a higher degree of disorder in the neighbouring *sn-1* chain, regardless of the charge set used.

Both the 2D-RDF and deuterium order parameter results indicate that use of the modified charge set reduces order in the *sn-1* chain for all three lipids, while only making a significant impact on the *sn-2* chains of DPPC and POPC. While considered separately in the previous analysis, the interdependence of the two chain behaviours should not be overlooked. Improvement in even one of the chains is sufficient to positively impact both the dynamics of the second chain and the overall membrane behaviour.

4. Conclusions

Following the work of Sonne et al. [31] we have extended and implemented a new charge set for a series of PC lipids, resulting in dramatic improvements in bulk lipid parameters. While the new force field does not adhere to the traditional CHARMM parameterisation strategy the clear improvement seen in lipid behaviour indicates that this new model may be used to simulate a membrane environment without the need for extensive force field development. This being said, some of the shortcomings of the current model may be ameliorated through full optimisation of the head group atoms including an examination of torsional potential energies.

All three lipids studied, DPPC, POPC and PDPC, exhibited experimentally valid bilayer behaviour. Both membrane width and area per lipid were seen to converge to experimental values relatively rapidly. The increased area per lipid induced by the modified charge set enabled increased water penetration, allowing the carbonyl group to become fully hydrated. Head group atom properties were seen to become more uniform with the modified charge set, indicating a more fluid and relaxed state. The biggest improvement, however, was seen in the behaviour of the hydrocarbon tails. All three lipids displayed increased hydrocarbon disorder across the width of the bilayer when using the modified charge set as indicated by reduced deuterium order parameters. Disorder was slightly over-estimated in the low carbon region, the implications of which are unknown. In

general the hydrocarbon tails were seen to occupy a broader range of conformations and ultimately adopt a more splayed and kinked conformation. Recent work has hi-lighted the impact of double bond parameterisation on both qualitative and quantitative membrane behaviour [71]. In the current model the CHARMM force field treats each double bond as a similar unit, regardless of its position within the hydrocarbon tail. It is likely that this simplistic approach is not sufficient to replicate experimental membrane behaviour. Further refinement of the alkenyl group parameters may serve to improve the localised behaviour of the hydrocarbon tails.

Our analysis shows that charge set selection is of critical importance to reproducing accurate membrane behaviour. In particular we have shown that the new charge set results in a significant improvement in bulk membrane properties over the original CHARMM27r charge set for all three lipids, implying that it may be applied as a general charge set for all phosphatidylcholines. This improvement allows us to extend our work to mixed biological systems and tensionless NPT ensembles, which was previously not possible.

Acknowledgements

The authors wish to thank the EU Marie Curie Transfer of Knowledge Programme for fellowship and project funding. We would also like to acknowledge the Institute for Information Technology and Advanced Computation (IITAC), the Higher Learning Authority (HEA) PRTLI scheme, the National Development Plan (NDP) and the Trinity Centre for High Performance Computing (TCHPC) for the provision of computational facilities and support. Further thanks goes to the Vattulainen group at the Tampere University of Technology, Finland, for generously providing pre-equilibrated hydrated membrane coordinates which served as the starting point for this work.

References

[1] P. van der Ploeg, H.J.C. Berendsen, Molecular dynamics of a bilayer membrane, Mol. Phys. 49 (1983) 233–248.
[2] J.J. Wendoloski, S.J. Kimatian, C.E. Schutt, F.R. Salemme, Molecular dynamics simulation of a phospholipid micelle, Science 243 (1989) 636–638.
[3] H. Heller, M. Schaefer, K. Schulten, Molecular dynamics simulation of a bilayer of 200 lipids in the gel and in the liquid crystal phase, J. Phys. Chem. 97 (1993) 8343–8360.
[4] D.P. Tieleman, S.J. Marrink, H.J. Berendsen, A computer perspective of membranes: molecular dynamics studies of lipid bilayer systems, Biochim. Biophys. Acta 1331 (1997) 235–270.
[5] M. Patra, M. Karttunen, M.T. Hyvönen, E. Falck, I. Vattulainen, Lipid bilayers driven to a wrong lane in molecular dynamics simulations by subtle changes in long-range electrostatic interactions, J. Phys. Chem., B 108 (2004) 4485–4494.
[6] S. Leekumjorn, A.K. Sum, Molecular characterization of gel and liquid-crystalline structures of fully hydrated POPC and POPE bilayers, J. Phys. Chem., B 111 (2007) 6026–6033.
[7] J.S. Hub, T. Salditt, M.C. Rheinstadter, B.L. de Groot, Short range order and collective dynamics of dmpc bilayers. A comparison between molecular dynamics simulations, X-ray, and neutron scattering experiments, Biophys. J. 93 (2007) 3156–3168.
[8] S. Ollila, M.T. Hyvönen, I. Vattulainen, Polyunsaturation in lipid membranes: dynamic properties and lateral pressure profiles, J. Phys. Chem., B 111 (2007) 3139–3150.
[9] M.H. Cheng, L.T. Liu, A.C. Saladino, Y. Xu, P. Tang, Molecular dynamics simulations of ternary membrane mixture: phosphatidylcholine, phosphatidic acid, and cholesterol, J. Phys. Chem., B 111 (2007) 14186–14192.
[10] J. Aittoniemi, P.S. Niemelä, M.T. Hyvönen, M. Karttunen, I. Vattulainen, Insight into the putative specific interactions between cholesterol, sphingomyelin, and palmitoyl–oleoyl phosphatidylcholine, Biophys. J. 92 (2007) 1125–1137.
[11] S. Leekumjorn, A.K. Sum, Molecular simulation study of structural and dynamic properties of mixed DPPC/DPPE bilayers, Biophys. J. 90 (2006) 3951–3965.
[12] W.L. Ash, M.R. Zlomislic, E.O. Oloo, D.P. Tieleman, Computer simulation of membrane proteins, Biochim. Biophys. Acta 1666 (2004) 158–189.
[13] P.S. Niemelä, S. Ollila, M.T. Hyvönen, M. Karttunen, I. Vattulainen, Assessing the nature of lipid raft membranes, PLOS Comput. Biol. 3 (2007) 304–312.
[14] D. Bemporad, C. Luttmann, J.W. Essex, Behaviour of small solutes and large drugs in a lipid bilayer from computer simulations, Biochim. Biophys. Acta 1718 (2005) 1–21.
[15] S. Baoukina, L. Monticelli, M. Amrein, D.P. Tieleman, The molecular mechanism of monolayer–bilayer transformations of lung surfactant from molecular dynamics simulations, Biophys. J. 93 (2007) 3775–3782.
[16] M.Ø. Jensen, O.G. Mouritsen, Lipids do influence protein function – The hydrophobic matching hypothesis revisited, Biochim. Biohys. Acta 1666 (2004) 205–226.
[17] R.S. Cantor, The lateral pressure profile in membranes: a physical mechanism of general anesthesia, Biochemistry 36 (1997) 2339–2344.
[18] A. Grossfield, S.E. Feller, M.C. Pitman, A role for direct interactions in the modulation of rhodopsin by ω-3 polyunsaturated lipids, Proc. Natl. Acad. Sci. U. S. A. 103 (2006) 4888–4893.
[19] A.V. Botelho, T. Huber, T.P. Sakmar, M.F. Brown, Curvature and hydrophobic forces drive oligomerization and modulate activity of rhodopsin in membranes, Biophys. J. 91 (2006) 4464–4477.
[20] J. Gullingsrud, K. Schulten, Lipid bilayer pressure profiles and mechanosensitive channel gating, Biophys. J. 86 (2004) 3496–3509.
[21] A.G. Lee, How lipids affect the activities of integral membrane proteins, Biochim. Biophys. Acta 1666 (2004) 62–87.
[22] S.E. Feller, A.D. Mackerell Jr., An improved empirical potential energy function for molecular simulations of phospholipids, J. Phys. Chem., B 104 (2000) 7510–7515.
[23] J.B. Klauda, B.R. Brooks, A.D. Mackerell Jr., R.M. Venable, R.W. Pastor, An ab initio study on the torsional surface of alkanes and its effect on molecular simulations of alkanes and a DPPC bilayer, J. Phys. Chem., B 109 (2005) 5300–5311.
[24] D.P. Tieleman, H.J.C. Berendsen, Molecular dynamics simulations of a fully hydrated dipalmitoylphosphatidylcholine bilayer with different macroscopic boundary conditions and parameters, J. Chem. Phys. 105 (1996) 4871–4880.
[25] J.F. Nagle, S. Tristram-Nagle, Structure of lipid bilayers, Biochim. Biophys. Acta 1469 (2000) 159–195.
[26] J.N. Sachs, H.I. Petrache, T.B. Woolf, Interpretation of small angle X-ray measurements guided by molecular dynamics simulations of lipid bilayers, Chem. Phys. Lipids 126 (2003) 211–223.
[27] R.W. Benz, F. Castro-Roman, D.J. Tobias, S.H. White, Experimental validation of molecular dynamics simulations of lipid bilayers: a new approach, Biophys. J. 88 (2005) 805–817.
[28] J.B. Klauda, N. Kucerka, B.R. Brooks, R.W. Pastor, J.F. Nagle, Simulation-based methods for interpreting X-ray data from lipid bilayers, Biophys. J. 90 (2006) 2796–2807.
[29] S.W. Chiu, M.M. Clark, E. Jakobsson, S. Subramaniam, L.H. Scott, Optimization of hydrocarbon chain interaction parameters: application to the simulation of fluid phase lipid bilayers, J. Phys. Chem., B 103 (1999) 6323–6327.
[30] X. Daura, A.E. Mark, W.F. Van Gunsteren, Parameterization of aliphatic CH_n united atoms of GROMOS96 force field, J. Comput. Chem. 19 (1998) 535–547.
[31] J. Sonne, M.Ø. Jensen, F.Y. Hansen, L. Hemmingsen, G.H. Peters, Reparameterization of all-atom dipalmitoylphosphatidylcholine lipid parameters enables simulation of fluid bilayers at zero tension, Biophys. J. 92 (2007) 4157–4167.
[32] J. Wang, R.M. Wolf, J.W. Caldwell, P.A. Kollman, D.A. Case, Development and testing of a general Amber force field, J. Comput. Chem. 25 (2004) 1157–1174.
[33] P. Cieplak, W.D. Cornell, C. Bayly, P.A. Kollman, Application of the multimolecule and multiconformational RESP methodology to biopolymers: charge derivation for DNA, RNA, and proteins, J. Comput. Chem. 16 (1995) 1357–1377.
[34] B. Jójárt, T.A.A. Martinek, Performance of the general Amber force field in modeling aqueous POPC membrane bilayers, J. Comput. Chem. 28 (2007) 2051–2058.
[35] S.E. Feller, R.W. Pastor, On simulating lipid bilayers with an applied surface tension: periodic boundary conditions and undulations, Biophys. J. 71 (1996) 1350–1355.
[36] S.W. Chiu, M. Clark, V. Balaji, S. Subramaniam, H.L. Scott, E. Jakobsson, Incorporation of surface tension into molecular dynamics simulation of an interface: a fluid phase lipid bilayer membrane, Biophys. J. 69 (1995) 1230–1245.
[37] S.E. Feller, D. Yin, R.W. Pastor, A.D. MacKerell Jr., Molecular dynamics simulation of unsaturated lipid bilayers at low hydration: parameterization and comparison with diffraction studies, Biophys. J. 73 (1997) 2269–2279.
[38] R.J. Mashl, H.L. Scott, S. Subramaniam, E. Jakobsson, Molecular simulation of dioleoylphosphatidylcholine lipid bilayers at differing levels of hydration, Biophys. J. 81 (2001) 3005–3015.
[39] O. Berger, O. Edholm, F. Jahnig, Molecular dynamics simulations of a fluid bilayer of dipalmitoylphosphatidylcholine at full hydration, constant pressure, and constant temperature, Biophys. J. 72 (1997) 2002–2013.
[40] F. Jahnig, What is the surface tension of a lipid bilayer membrane? Biophys. J. 71 (1996) 1348–1349.
[41] S.J. Marrink, A.E. Mark, Effect of undulations on surface tension in simulated bilayers, J. Phys. Chem., B 105 (2001) 6122–6127.
[42] T. Huber, K. Rajamoorthi, V.F. Kurze, K. Beyer, M.F. Brown, Structure of docosahexaenoic acid-containing phospholipid bilayers as studied by ^2H NMR and molecular dynamics simulations, J. Am. Chem. Soc. 124 (2002) 298–309.
[43] E. Lindahl, O. Edholm, Mesoscopic undulations and thickness fluctuations in lipid bilayers from molecular dynamics simulations, Biophys. J. 79 (2000) 426–433.
[44] J. Wohlert, O. Edholm, The range and shielding of dipole–dipole interactions in phospholipid bilayers, Biophys. J. 87 (2004) 2433–2445.
[45] M. Patra, M. Karttunen, M.T. Hyvönen, E. Falck, P. Lindqvist, I. Vattulainen, Molecular dynamics simulations of lipid bilayers: major artifacts due to truncating electrostatic interactions, Biophys. J. 84 (2003) 3636–3645.
[46] W. Humphrey, A. Dalke, K. Schulten, VMD – visual molecular dynamics, J. Mol. Graph. 14 (1996) 33–38.
[47] W.L. Jorgensen, J. Chandrasekhar, J.D. Madura, R.W. Impey, M.L. Klein, Comparison of simple potential functions for simulating liquid water, J. Chem. Phys. 79 (1983) 926–935.

[48] N. Foloppe, A.D. Mackerell Jr., All-atom empirical force field for nucleic acids: I. parameter optimization based on small molecule and condensed phase macromolecular target data, J. Comput. Chem. 21 (2000) 86–104.
[49] J.C. Phillips, R. Braun, W. Wang, J. Gumbart, E. Tajkhorshid, E. Villa, C. Chipot, R.D. Skeel, L. Kalé, K. Schulten, Scalable molecular dynamics with NAMD, J. Comput. Chem. 26 (2005) 1781–1802.
[50] T. Darden, D. York, L. Pedersen, Particle mesh Ewald: An Nlog(N) method for Ewald sums in large systems, J. Chem. Phys. 98 (1993) 10089–10092.
[51] U. Essmann, L. Perera, M.L. Berkowitz, T. Darden, H. Lee, L.G. Pedersen, A smooth particle mesh Ewald method, J. Chem. Phys. 103 (1995) 8577–8593.
[52] R.L. Biltonen, D. Lichtenberg, The use of differential scanning calorimetry as a tool to characterize liposome preparation, Chem. Phys. Lipids 64 (1993) 129–142.
[53] S.E. Feller, Y. Zhang, R.W. Pastor, B.R. Brooks, Constant pressure molecular dynamics simulation: the Langevin piston method, J. Chem. Phys. 103 (1995) 4613–4621.
[54] G.J. Martyna, D.J. Tobias, M.L. Klein, Constant pressure molecular dynamics algorithms, J. Chem. Phys. 101 (1994) 4177–4189.
[55] D. Van Der Spoel, E. Lindahl, B. Hess, G. Groenhof, A.E. Mark, H.J. Berendsen, Gromacs: fast, flexible, and free, J. Comput. Chem. 26 (2005) 1701–1718.
[56] J. Stone, *An efficient library for parallel ray tracing and animation*, Master's thesis, Computer Science Department, University of Missouri-Rolla (April 1998).
[57] S. Leekumjorn, A.K. Sum, Molecular studies of the gel to liquid-crystalline phase transition for fully hydrated DPPC and DPPE bilayers, Biochim. Biophys. Acta 1768 (2007) 354–365.
[58] S.E. Feller, R.W. Pastor, Constant surface tension simulations of lipid bilayers: The sensitivity of surface areas and compressibilities, J. Chem. Phys. 111 (1999) 1281–1287.
[59] M. Patra, E. Salonen, E. Terama, I. Vattulainen, R. Faller, B.W. Lee, J. Holopainen, M. Karttunen, Under the influence of alcohol: the effect of ethanol and methanol on lipid bilayers, Biophys. J. 90 (2006) 1121–1135.
[60] M.C. Wiener, S.H. White, Structure of a fluid dioleoylphosphatidylcholine bilayer determined by joint refinement of X-ray and neutron diffraction data. iii. complete structure. Biophys. J. 61 (1992) 434–447.
[61] D.L. Lynch, P.H. Reggio, Molecular dynamics simulations of the endocannabinoid n-arachidonoylethanolamine (anandamide) in a phospholipid bilayer: probing structure and dynamics, J. Med. Chem. 48 (2005) 4824–4833.
[62] B.W. Koenig, H.H. Strey, K. Gawrisch, Membrane lateral compressibility determined by NMR and X-ray diffraction: effect of acyl chain polyunsaturation, Biophys. J. 73 (1997) 1954–1966.
[63] H.I. Petrache, A. Salmon, M.F. Brown, Structural properties of docosahexaenoyl phospholipid bilayers investigated by solid-state ^{2}H NMR spectroscopy, J. Am. Chem. Soc. 123 (2001) 12611–12622.
[64] H. Akutsu, T. Nagamori, Conformational analysis of the polar head group in phosphatidylcholine bilayers: a structural change induced by cations, Biochemistry 30 (1991) 4510–4516.
[65] J.N. Sachs, H. Nanda, H.I. Petrache, T.B. Woolf, Changes in phosphatidylcholine headgroup tilt and water order induced by monovalent salts: molecular dynamics simulations, Biophys. J. 86 (2004) 3772–3782.
[66] A. Seelig, J. Seelig, Effect of a single cis double bond on the structure of a phospholipid bilayer, Biochemistry. 16 (1977) 45–50.
[67] A. Seelig, J. Seelig, Lipid conformation in model membranes and biological membranes, Q. Rev. Biophys. 13 (1980) 19–61.
[68] J.H. Davis, M. Bloom, K.W. Butler, I.C.P. Smith, The temperature dependence of molecular order and the influence of cholesterol in acholeplasma laidlawii membranes, Biochim. Biophys. Acta 597 (1980) 477–491.
[69] M. Lafleur, B. Fine, E. Sternin, P.R. Cullis, M. Bloom, Smoothed orientational order profile of lipid bilayers by ^{2}H-nuclear magnetic resonance, Biophys. J. 56 (1989) 1037–1041.
[70] L. Rosso, I.R. Gould, Structure and dynamics of phospholipid bilayers using recently developed general all-atom force fields, J. Comput. Chem. 29 (2008) 24–37.
[71] H. Martinez-Seara, T. Róg, M. Karttunen, R. Reigada, I. Vattulainen, Influence of cis double-bond parametrization on lipid membrane properties: how seemingly insignificant details in force-field change even qualitative trends, J. Chem. Phys. 129 (2008) 105103–105110.
[72] N. Kučerka, S. Tristram-Nagle, J.F. Nagle, Structure of fully hydrated fluid phase lipid bilayers with monounsaturated chains, J. Membr. Biol. 208 (2005) 193–202.
[73] A. Seelig, N. Waespe-Šarčevic, Molecular order in cis and trans unsaturated phospholipid bilayers, Biochemistry 17 (1978) 3310–3315.
[74] B. Perly, I.C.P. Smith, H.C. Jarrell, Effects of the replacement of a double bond by a cyclopropane ring in phosphatidylethanolamines: a ^{2}H NMR study of phase transitions and molecular organization, Biochemistry 24 (1985) 1055–1063.